Elastic moduli of polyelectrolyte multilayer films regulate endothelium-blood interaction under dynamic conditions

Imbir, Gabriela; Trembecka-Wójciga, Klaudia; Ozga, Piotr; Schirhagl, Romana; Mzyk, Aldona

Published in:
Colloids and Surfaces B: Biointerfaces

DOI:
10.1016/j.colsurfb.2023.113269

Publication date:
2023

Colloids and Surfaces B: Biointerfaces 225 (2023) 113269

Contents lists available at ScienceDirect

Colloids and Surfaces B: Biointerfaces

journal homepage: www.elsevier.com/locate/colsurfb

Elastic moduli of polyelectrolyte multilayer films regulate endothelium-blood interaction under dynamic conditions

Gabriela Imbir [a,b,*,1], Klaudia Trembecka-Wójciga [a], Piotr Ozga [a], Romana Schirhagl [c], Aldona Mzyk [a,c,*,1]

[a] Institute of Metallurgy and Materials Science Polish Academy of Sciences, 25 Reymonta Street, 30-059 Cracow, Poland
[b] Institute of Nuclear Physics Polish Academy of Sciences, 152 Radzikowski Street, 31-342 Cracow, Poland
[c] Groningen University, University Medical Center Groningen, Antonius Deusinglaan 1, 9713 AV Groningen, the Netherlands

ARTICLE INFO

Keywords:
Endothelial cells
Polyelectrolyte multilayer
Nanodiamond magnetometry
Blood-material interaction
T1 relaxometry

ABSTRACT

A broad spectrum of biomaterials has been explored in order to design cardiovascular implants of sufficient hemocompatibility. Most of them were extensively tested for the ability to facilitate repopulation by patient cells. It was shown that stiffness, surface roughness, or hydrophilicity of polyelectrolyte films have an impact on adhesion, proliferation, and differentiation of cells. At the same time, it is still unknown how these properties influence cell functionality and as a consequence interactions with blood components under dynamic conditions. In this study, we aimed to determine the impact of chemical cross-linking of Chitosan (Chi) and Chrondroitin Sulphate (CS) on endothelium-blood cross-talk. We have found that the morphology of the endothelium monolayer was not altered by changes in coating properties. However, free radical generation by endothelial cells varied depending on the elastic properties of the coating. Simultaneously, we have observed a significant decrease in the level of adhering and circulating active platelets as well as aggregates when the endothelium monolayer was formed on stiffer films than on the other coating variants. Moreover, the same type of films has promoted significantly higher adhesion of blood morphotic elements when they were not functionalized by endothelium. The observed changes in hemocompatibility indicate the importance of a design of coatings that will promote cellularization *in vivo* in a relatively short time and which will regulate cell function.

1. Introduction

Modern tissue engineering offers a variety of methods to restore functionality of damaged tissue. A broad spectrum of materials such as metals, polymers or ceramics was explored in order to design implants, which could be efficiently populated by patient cells [1]. Acellular, animal derived tissues have been suggested as a promising alternative to synthetic scaffolds [2]. Nevertheless, beside removal of cellular component currently available acellularization methods lead to the degradation of the extracellular component of the tissue [2]. Therefore, animal derived scaffolds require post-acellularization treatment in order to restore their structure and functions. Polyelectrolyte multilayer coatings (PEMs) that consist of polymers from a natural origin seem to be a suitable for their reconstruction. Beside excellent biocompatibility, PEMs are characterized by easily adjustable physico-chemical properties [3]. Yamanlar et al. have shown that surface functionalization with PEMs can modulate the ability of implants to release proteins, drugs or growth factors in a controlled manner [3]. It has also been proved that PEMs can regulate proteins adsorption from body fluids and cellular responses such as adhesion, proliferation and differentiation, which are crucial for an integration of the implant with the patient body [4]. Control of protein adsorption and dependent cell behaviour is possible due to tuning PEMs physico-chemical properties [5]. PEMs with various characteristics were obtained by chemical cross-linking, incorporation of nanoparticles or changes of pH during the film build-up process [4, 6–8]. It has been reported that hydrophilicity, type of functional groups and surface charge influence the cell adhesion [9]. Schneider et al. have indicated that also PEMs mechanical properties, i.e., stiffness have an impact on the cell response [10]. So far, PEMs have been suggested as coatings mainly for titanium-based bone implants [11] or the

* Correspondence to: Institute of Nuclear Physics 152 Radzikowskiego Street, 31-342 Cracow and Institute of Metallurgy and Materials Science Polish Academy of Sciences, 25 Reymonta Street, 30-059 Cracow, Poland.
E-mail addresses: gabi.imbir@gmail.com (G. Imbir), a.i.mzyk@umcg.nl (A. Mzyk).
[1] These authors contributed equally.

https://doi.org/10.1016/j.colsurfb.2023.113269
Received 19 January 2023; Received in revised form 2 March 2023; Accepted 13 March 2023
Available online 15 March 2023

electrospun scaffolds [12] to improve osseointegration, while the cardiovascular field needs to be further explored. Kerdjoudj et al. have shown the potential of PEMs to be applied as coatings for vascular cryopreserved arteries [13]. They have indicated that functionalization of tissue with PEMs helped to restore its biomechanical properties. They have also observed that functional groups exposed on the surface of PEMs induced re-endothelialisation of modified arteries. Gribova et al., found that sulfonate groups (SO_3^-) may play a crucial role in endothelial monolayer formation [4]. Nevertheless, none of the research groups have investigated if the formed endothelial layer provides implants with the proper functionality when it stays in contact with blood. In the case of cardiovascular implants, it is important that endothelial cells prevent undesired activation of the coagulation cascade and platelets adhesion/aggregation. Under the physiological conditions, the endothelium produces enzymes, nitric oxide (*NO) and prostacyclin, which are responsible for the inhibition of platelets activation. In a pathological stage such as hypertension or dyslipidemia, accumulation of low-density lipoprotein (LDL) and an increase of tissue rigidity cause a decrease of *NO levels, which next leads to triggering the inflammatory pathway and reinforcing platelet adhesion. During the inflammatory processes, activated platelets interact with P-selectin and E-selectin, which are expressed on the endothelial surface [14]. The exact mechanisms behind cell rigidity sensing and free radicals (FRs – molecules with unpaired electrons, including some reactive oxygen and nitrogen species) generation are poorly understood.

In our previous research [15], we have made a very first attempt to understand PEMs interaction with blood under flow conditions. The obtained results enable understanding of how the physico-chemical properties of PEMs modulate interaction with blood plasma proteins and the morphotic elements. We have shown that the Chi/CS system is a promising material for cardiovascular implants. Therefore, in this study, the Chi/CS coating has been further developed in order to support an efficient endothelialization. Herein, we have investigated how PEMs determine interactions between endothelial monolayers and blood morphotic elements.

2. Materials and methods

Chitosan and Chondroitin Sulphate were acquired from Sigma-Aldrich (Saint Louis, Missouri, USA). Human Umbilical Vein Endothelial Cells Medium and Supplements were purchased from Promocell (Heidelberg, Germany). Alexa Fluor 488 phalloidin and DAPI were acquired from Life Technologies (Carlsbad, CA, USA). Sodium Dodecyl Sulphate (SDS) was purchased from Sigma-Aldrich. The impact-R device for the cone and plate test was purchased from DiaMed Ltd. Activation of blood coagulation was analysed using confocal laser scanning microscopy (CLSM) and flow cytometry. Following antibodies were applied for flow cytometry: anti-PAC-1-FITC, anti-CD62P-PE, anti-CD61-PerCP, anti-CD14-PerCP supplied by BD Science (San Jose, CA, USA). For the CLSM observations anti-CD45 PE, anti-CD62P FITC and anti-vWF antibodies were purchased from BioLegend (San Diego, CA, USA). Isotype controls (anti-IgG1-PE, anti-IgM-FITC and anti-IgG1-FITC) were supplied by BD Bioscience. A ZymuphenMP-activity ELISA kit from Hyphen Biomed Eragny, France was applied in a microparticles concentration investigation. The nanodiamonds used for T1 relaxometry were bought from Adamas Nanotechnologies, NC, USA.

2.1. Preparation of polyelectrolyte multilayer films

Coatings were deposited on polyurethane disks with a diameter of 14.4 mm and a thickness of 2 mm. Polyurethane (PU) was selected as a substrate for the polyelectrolyte films deposition as well as a control for our experiments due to its wide application in cardiovascular devices. Polyelectrolyte multilayer films (PEMs) were manufactured using a "layer-by-layer" method. Due to its insolubility in water, chitosan (Chi) was pre-dissolved in 0.1 M acetic acid. The final concentration of both chitosan and chondroitin sulphate (CS) was 0.5 mg/mL Solutions were prepared in 0.15 M sodium chloride (NaCl) with a pH set at 5.5. Coatings were formed using an automatic dipping machine. The substrate was immersed in cationic and ionic polyelectrolyte solutions for 8 min each. In between deposition steps, the sample was rinsed with 0.15 M NaCl solution of pH 7.4 to remove excess of non-bonded polymer chains. The process was repeated until the 24 bilayers were achieved. This number of bilayers assures homogeneous coating of the substrate's surface.

The films were cross-linked with N-hydroxysulphosuccinimide (NHS) and 1-ethyl-3-(3-dimethylaminopropyl)carbodiimide (EDC) in order to limit polyelectrolytes inter-diffusion and therefore stabilise the coating structure. NHS (22 mg/mL) and EDC (100 mg/mL) were separately dissolved in sodium chloride of pH 6 and mixed in a 1:1 ratio. Coatings were kept in a cross-linking solution at 4 °C for 18 h. In the final step, the outermost layer of fibronectin (0.05 mg/mL) was deposited on PEMs to improve cell adhesion. Table 1 presents all variants of the prepared coating.

2.2. Physico-chemical properties of films

The film build up, thickness and stability were evaluated based on the QCM-D measurements. The details of the experiment were described in our previous paper [15].

The surface morphology of the coatings were analysed based on a series of images obtained from Atomic Force Microscopy (Innova Bruker). The measurements were carried out at room temperature in tapping mode using MLCT C silicon nitride tips (Bruker). Collected data was processed with the Nanoscope 1.40 Analysis Software.

The evaluation of PEMs stiffness was performed by AFM in nano-indentation mode. The measurements were carried out in 0.15 M NaCl set at pH 7.4 using borosilicate sphere-tipped cantilever with a radius of 2.5 μm and a nominal spring constant of 60 mN/m. For the indentation curve from 30 to 100 nm indentation depth, the Hertz model was applied. Two indentation measurements were performed in six different positions for each analysed sample. The Young Moduli were calculated based on the force-indentation curves fitted with the least-squares method.

A static contact angle was evaluated by the sessile drop method using a contact angle goniometer equipped with the automatic dosing system and camera (DSA100, Kruss). The deionized water was used as a liquid. Ten measurements were made for each coating type.

The amount of adsorbed fibronectin was determined using a Qubit® Protein Assay Kit and a Qubit® fluorometer according to the manufacturer's guidelines. Prior protein concentration measurements, samples were treated with 0.2 % of Sodium Dodecyl Sulphate (SDS) in order to transfer adsorbed fibronectin into solution. Data analysis was performed using the OriginPro2018 software.

2.3. Film endothelialization

Human Umbilical Vein Endothelial Cells (HUVECs) were cultured in 25 cm^2 flasks under standard conditions (37 °C and 5 % CO_2). When cells reached 80 % confluency they were detached from the flask surface with the trypsin/EDTA (1:1 concentration) and were seeded on the samples with a density of $4{\cdot}10^4$ cells per cm^2. HUVECs were cultured on the materials for 4 days and thereafter fixed with 4 % paraformaldehyde in order to evaluate cell morphology or were used in the

Table 1
Fabricated PEM coatings.

Coating name	Cross-linking with NHS/EDC	Outermost layer
(Chi/CS)24 non cross	No	fibronectin
(Chi/CS)24 1x cross	after 24 bilayers	fibronectin
(Chi/CS)24 2x cross	after each 12 bilayers	fibronectin
(Chi/CS)24 4x cross	After each 6 bilayers	fibronectin

hemocompatibility assay as well as in T1 relaxometry.

Cell number and morphology were analysed using a confocal laser scanning microscopy (LSM Exciter 5, Zeiss). For this purpose, cells were stained with Alexa Fluor 488 phalloidin to determine distribution of actin filaments, whereas DAPI (4′,6-diamidino-2-phenylindole) stain was used to visualise nuclei. Observations were carried out at a 20x magnification. The cell number and area were calculated with the ImageJ software. Based on the obtained data, also the shape index, which describes cell roundness, was determined.

2.4. PEMs influence on free radical generation by the endothelium

The free radical (FRs) generation by HUVECs was evaluated based on data obtained from T1 relaxometry measurements. The fluorescent oxygen-terminated nanodiamond particles (FNDs) with a mean hydrodynamic diameter of 70 nm and a flake-like structure were used as probes characterised in our previous work [16–18]. These FNDs are manufactured by high-pressure high-temperature (HPHT) synthesis followed by irradiation and high temperature annealing. Each particle contained about 300 nitrogen vacancy (NV^-) centers (determined by the producer).

Prior to T_1 relaxometry, endothelial cells were treated with FNDs at a concentration of 2 μg/mL for 4-hours at 37 °C and 5 % CO_2. Then cells were subjected to the shearing conditions at 1800s^{-1} and the T1s were recorded. The NV^- centers were pumped to the bright ground state with a green laser pulse. Afterwards, we probed if the NV^- centers were still there or had returned to the darker equilibrium state. This process gets shortened in presence of FRs in the surrounding of the nanodiamond probe, which means that the relaxation time (=T_1) reveals the radical concentration. The experiments were carried out by using an in house made magnetometry setup, described elsewhere [16]. The collected data was processed using our original MatLab R2018b software.

2.5. Blood interaction with cellularized PEMs

Blood interaction with cellularized films was analysed under *in vitro* dynamic conditions. Whole human blood was acquired from the Regional Donation Centre in Krakow. Dynamic tests were performed under high shear force (300 s, shear rate of 1800 s^{-1}) using a cone-plate tester. Blood was activated with adenosine diphosphate (ADP, concentration 20 μM) for 5 min, which was assigned as a control for the capacity of activated platelets. According to the manufacturer's recommendations, 130 μL of blood were used for each sample. After the test, blood was immediately sampled for further evaluation. Film surface coverage by blood morphotic elements was determined using confocal laser scanning microscopy (CLSM). Blood morphotic elements on the surface of the samples were stained with antibodies conjugated with fluorochromes: anti-CD45, anti-CD62P and von Willebrand factor (vWF). Flow cytometry analysis aimed to assess platelet activation and aggregate formation in blood after contact with the material. Therefore, antibodies PAC-1-FITC, CD62P-PE and PerCP-CD61 were applied. Each antibody was diluted in PBS set at pH 7.4 and then mixed with the blood. In order to measure thrombotic activity, the blood was centrifuged for 5 min, thereafter separated plasma was collected. Thrombogenic potential was investigated by a ZymuphenMP-activity ELISA kit, according to the manufacturer's instruction[19].

2.6. Statistical analysis

Statistical analysis was performed using OriginPro 2018. The data was treated with an ANOVA and post hoc Tukey test, with * $p < 0.05$, ** $p < 0.01$, *** $p < 0.001$, * ** * $p < 0.0001$ considered as significant.

3. Results and discussion

3.1. Physicochemical properties of films

The film build up, thickness and stability were evaluated based on the QCM-D measurements. We have already discussed the results in our previous paper [15], where we stated that Chi/CS coating grows exponentially as a number of layers increases, which is caused by inter-diffusion within the multilayer. We have found that cross-linked coatings decreased their thickness by ~18 % compared to non cross-linked. Moreover, after 14 days of incubation in physiological salt, film thickness increased by ~18 % and ~4 % over time for non cross-linked and cross-linked, respectively.

The surface morphology of PEMs was determined based on the images obtained from the atomic force microscope. The AFM micrographs showed the presence of each film covered by fibronectin (Supplementary Information Fig. 1). It was found that roughness of Chi/CS films decreased after cross-linking (Fig. 1A). Both cross-linked and double cross-linked coatings showed similar roughness. Results obtained from nanoindentation indicated differences between the elastic moduli of films. Chemical cross-linking of PEMs caused a significant increase in its Young modulus (Fig. 1B). It was found that 2x cross-linked films were characterised by four times higher elasticity moduli (42.5 ± 2.4 kPa) than unmodified Chi/CS coatings, whereas the elastic moduli of 4x cross-linked PEMs increased almost 10 times [6,7,15].

The results of the contact angle measurements show a significant difference between wettability of unmodified and cross-linked Chi/CS films. The Chi/CS hydrophilicity increased after NHS/EDC treatment due to new bonds formed between free functional groups and decreased inter-diffusion within the film. It was found that 1x cross-linked film resulted in similar surface contact angle as 2x cross-linked and 4x cross-linked variants (Fig. 2A). The strong hydrophilic character of cross-linked films results in the presence of sulphate (SO_3^-) and carboxylic surface groups (COO^-) [15,20,21].

Finally, the protein assay provided information about the concentration of fibronectin that was adsorbed to variants of the Chi/CS film. The amount of fibronectin found on the 2x cross-linked surface was significantly lower compared with the unmodified film. The 2x cross-linked and 4x cross-linked films adsorbed a similar amount of fibronectin [8,15,21].

3.2. Film physicochemical properties influence endothelialization process

The effect of the coating type on endothelial cell morphology was evaluated based on the distribution of the actin filaments and localization of nuclei. Cells were forming a monolayer on all coating variants (Fig. 3). The cell surface area was determined based on immunofluorescence analysis. It was found that cells which are growing on the 1x cross-linked films have slightly smaller surface area than cells on the other type of coatings (Fig. 4A). It was an effect of the higher cell density on 1x cross-linked films. Cell elongation was determined based on a calculated shape index (SI) (Fig. 4B), which is defined as:

$$SI = \frac{4\pi A}{p^2} \quad (1)$$

where A is a cell area and p is a cell perimeter. SI values range from 0 to unity, where unity indicates cell roundness. The smallest SI value (0.54 ± 0.02) was found for cells on the 1x cross-linked films. There was no significant difference between the SI of cells growing on non-cross-linked, 2x and 4x cross-linked coatings.

The physico-chemical properties of polyelectrolyte multilayer coatings play a key role in the regulation of cell adhesion, proliferation and differentiation [6]. Mhamdi et al. showed that PEMs with lower contact angle indicate a higher adhesion rate [22]. They also demonstrated that a decrease in surface roughness promoted cell adhesion and

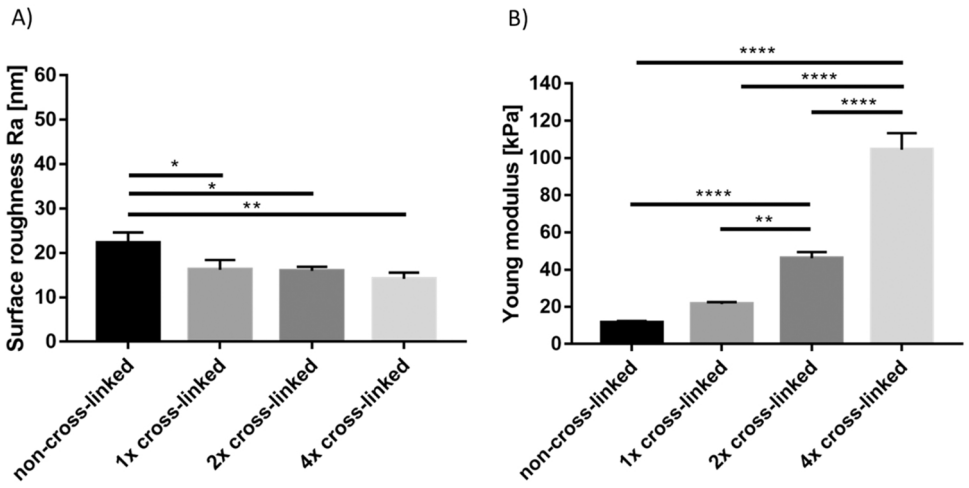

Fig. 1. A) Surface roughness and B) Young Modulus of Chi/CS coating variants. Data represent mean±SD, * $p < 0.05$, ** $p < 0.01$, *** $p < 0.001$, **** $p < 0.0001$.

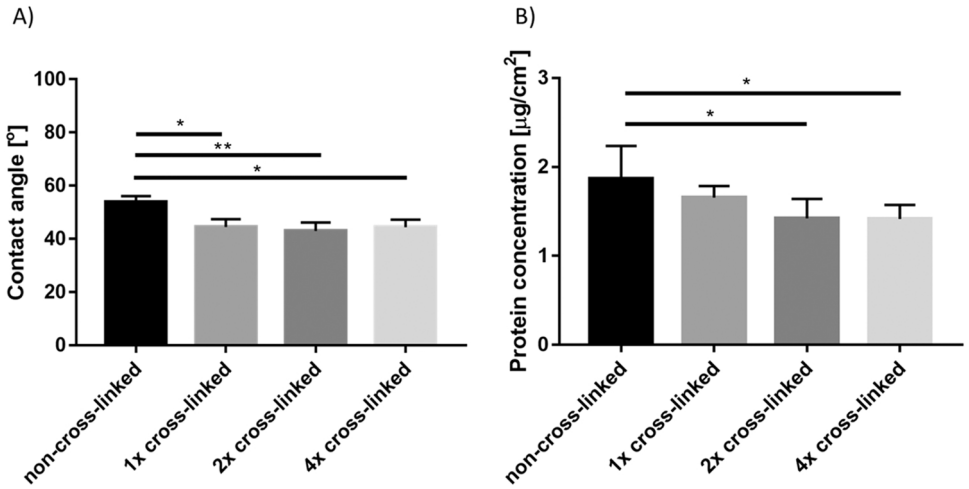

Fig. 2. A) Contact angle and B) concentration of fibronectin deposited on PEMs. Data represent mean ± SD, * $p < 0.05$, ** $p < 0.01$, *** $p < 0.001$, **** $p < 0.0001$.

proliferation, whereas its higher values hampered these processes. Cells also have an ability to sense stiffness of their environment [23]. Clinical investigations have shown that the small diameter vessels are as soft as 1 kPa, while vessels such as the aorta are as stiff as 20 kPa but can reach up to 70 kPa due to ageing or cardiovascular diseases [23]. Studies presented by Krishnan et al. demonstrated that the substrate stiffening has a negative impact on the endothelium function. The stiffness causes remodelling of the cytoskeleton by creating the actin stress fibres. Induced mechanical responses on the stiff substrates can activate the cell membrane stress-sensitive ion channels or could lead to conformational changes of proteins [23–25]. The stiffness of single endothelial cells (EC) increases with substrate stiffness however, in the tissue structure the stiffness may be different due to cell-cell interaction. High stiffness causes a decrease in the cell-cell interaction, thus cell-cell junctions are loose. Thereafter, the ECs form gaps, which in turn increase the cell permeability and results in endothelium dysfunction [26]. In this study, we have compared endothelium morphology and function on PEMs with an elastic modulus in the physiological range of 10 kPa-100 kPa. The surface chemistry, roughness and wettability were very similar for all obtained PEMs. The only detected significant differences concerned the Young Modulus. Within this elasticity range and for the given surface roughness, the formed EC monolayers did not differ. We have not observed gaps between cells and any discrepancies in their morphology. Similarly, Hu et al. examined this phenomenon for ECs growing on a Poly-L-lysine/ methacrylated hyaluronic acid (PLL/HA-MA) film, cross-linked with MMP peptide to control the stiffness. They have found that the morphology of endothelial monolayers did not differ on film variants with a stiffness in the range of 80 kPa-600 kPa, but there was a discrepancy in the endothelium function. Treatment with thrombin had no effect on ECs growing on coatings with adaptive mechanical properties, which resulted in disruption of the cell monolayer formed on the stiffer films. They have also performed an anticoagulant test, which showed that films with adaptive stiffness indicate lower platelet adhesion and shorter blood coagulation time compared to stiffer coatings [27].

3.3. PEMs influence on the free radical generation by the endothelium

Effect of the coating type on the generation of free radicals by endothelial cells was evaluated based on T1 relaxometry measurements. T1 values are inversely proportional to the free radical concentration near the nanodiamond sensor. It means that a decrease in T1s indicates an increase in the free radical concentration. In this study it has been found that gradual cross-linking of the coating resulted in a systematic decrease in T1 values. However, it has not been observed anymore after the 4x cross-linking. Then the T1 value has slightly increased but not significantly compared to the 2x cross-linked variant. Hu et al. have observed that ECs on softer PEMs produced more NO*, tissue

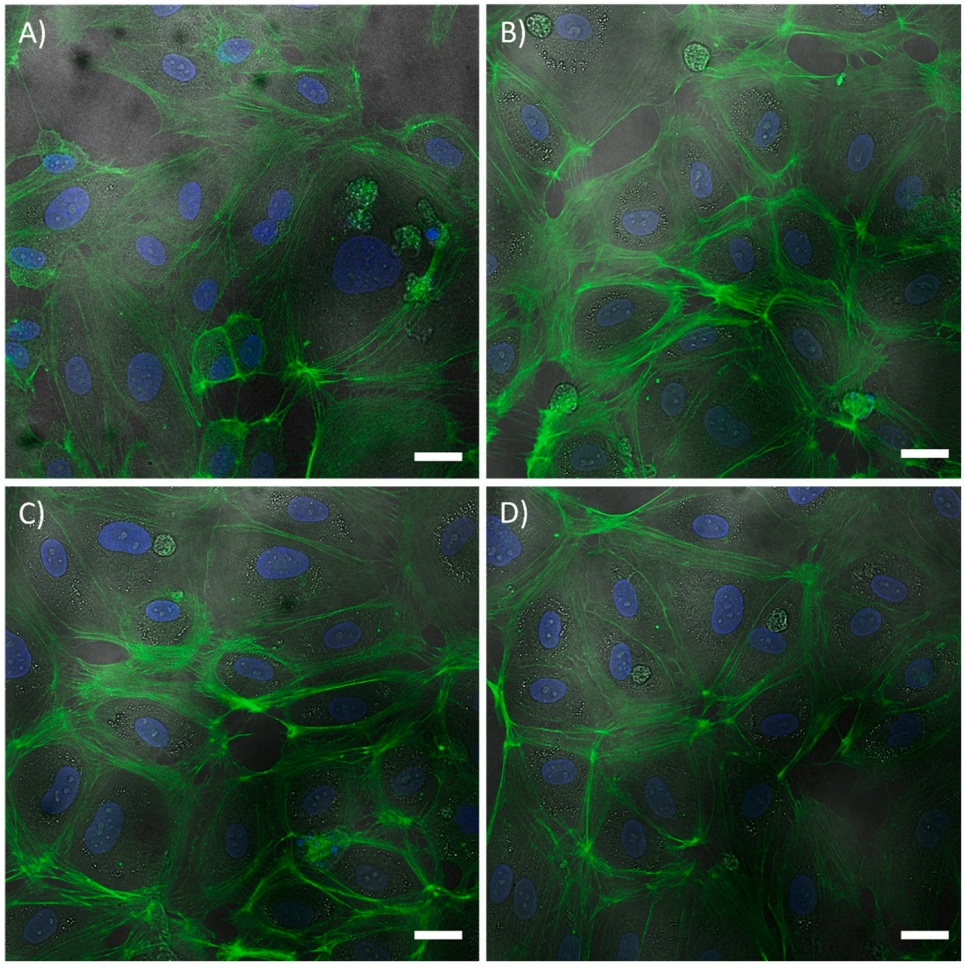

Fig. 3. Cell morphology on variants of 24 bilayer Chi/CS coating: A) non cross-linked, B) 1x cross-linked, C) 2x cross-linked and D) 4x cross-linked. The scale bar is 20 μm.

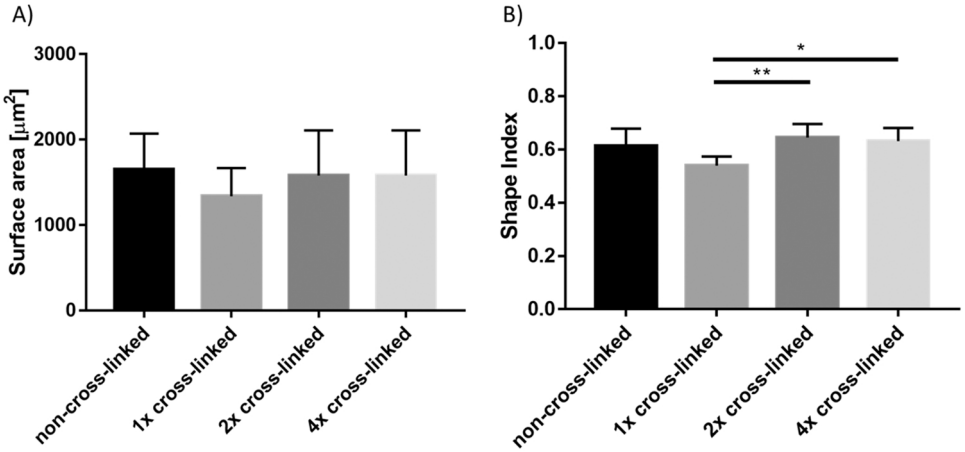

Fig. 4. Quantitative analysis of HUVECs morphology: A) cell surface area and B) shape index. The data represents mean±SD, * $p < 0.05$, ** $p < 0.01$, *** $p < 0.001$, **** $p < 0.0001$.

plasminogen activator tPA and prostacyclin PGI_2 than cells on the stiffer coatings [27].

3.4. Blood interaction with cellularized PEMs

Changes in blood quality were determined based on a comparison of parameters such as the number of the activated platelets, formed aggregates and microparticles. These hemocompatibility indicators were presented as a function of the number of initial platelets (PLT, Figs 5 and 6). Its high level demonstrates that only a small percentage of platelets was consumed in thrombogenesis. In this study, the platelet consumption was similar for most of the variants, except for the 2x and 4x cross-

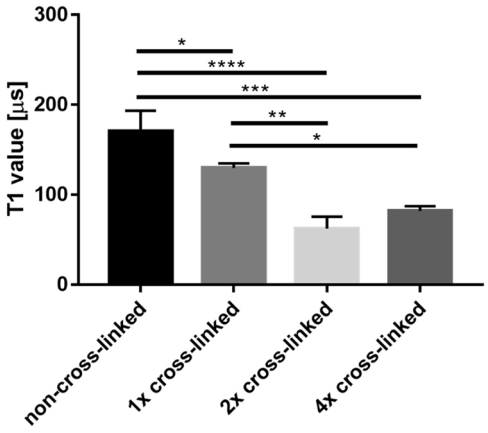

Fig. 5. T1 relaxation time measured in HUVECs growing on non cross-linked, 1x cross-linked, 2x cross-linked or 4x cross-linked PEMs. The data represents mean±SD, * $p < 0.05$, ** $p < 0.01$, * ** $p < 0.001$, * ** * $p < 0.0001$.

linked films as well as coating functionalized with fibronectin (FN) and populated by HUVECs.

The Selectin-P protein is a marker of platelet activation in thrombogenic or inflammatory processes. The highest platelet activation has been found in blood taken from above the 1x cross-linked film without cells (P-selectin$^+$, Fig. 6A). Contrarily, contact with cellularized 2x or 4x cross-linked coatings resulted in the lowest number of activated platelets. Surprisingly, the same variants without HUVECs led to a similar expression of the P-selectin marker. Furthermore, for these samples the platelet activation was comparable with the level obtained for the fibronectin control with cells.

The activated platelets tend to aggregate with each other and with leukocytes, which leads to blood clot formation. In this study, the lowest platelet aggregation (AGG, Fig. 6B) was found for blood sampled from above of the 2x and 4x cross-linked coatings, both cellularized and without cells. The unmodified and 1x cross-linked films both with and without HUVECs triggered formation of a similar number of the platelet-based aggregates. The number of leukocyte-platelet aggregates (AGG LUC-PLT) interacting with the endothelial cells is a good indicator of endothelial monolayer functionality and was used in this study (Fig. 6C). Similar to other investigated parameters, the contribution of monocyte-platelet aggregates was the lowest in blood that stayed in contact with 2x and 4x cross-linked for both cellularized and non-cellularized coatings. Whereas the cell-free 1x cross-linked films triggered the highest aggregate formation among Chi/CS variants.

The microparticles represent the fragments of the cell membrane, which are released into the bloodstream. Their excessive presence could indirectly cause aggregation of active platelets. Thus, monitoring their

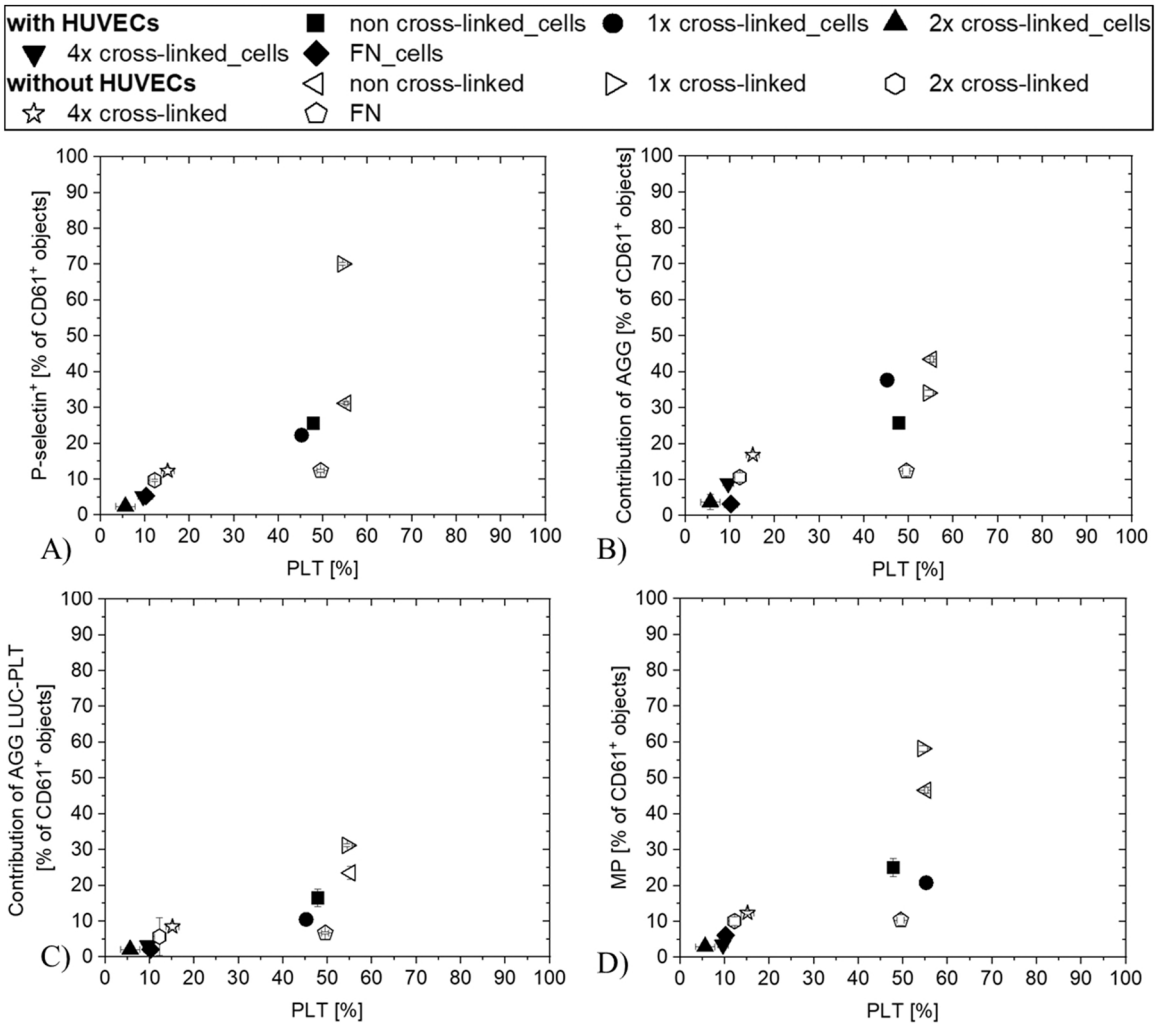

Fig. 6. Blood quality assessment based on A) the percentage of P-selectin positive objects (P-selectin$^+$), B) the contribution of platelet-based aggregates (AGG), C) the percentage of monocyte-platelet aggregates (AGG-LUC) and D) microparticles (MP) as a function of the initial amount of platelets (PLT). Data is represented by mean±SD.

level is crucial for hemocompatibility evaluation. The highest contribution of microparticles (MP) was observed in blood exposed to the 1x cross-linked films without HUVECs (Fig. 6D). It has been found that contact of blood with the 2x or 4x cross-linked films resulted in the lowest number of microparticles, regardless of the presence of cells.

Beside changes in blood parameters, we have also studied events that took place at the PEMs-blood interface (Fig. 7). Herein, we have determined how many active platelets and aggregates adhered to the surface of films. It has been found that 1x cross-linked coatings with HUVECs presented a smaller contribution of the P-selectin positive objects compared to films without cells (Fig. 7A). Contrary, the unmodified film without cells indicated lower active platelet adhesion than the same variant with cells.

The von-Willebrand Factor (VWF) is an essential protein involved in thrombus formation not only with respect to maintaining platelet adhesion but also as platelet-platelet cohesion or aggregation. Regardless of the presence of HUVECs, the unmodified films promoted adhesion of the same number of the VWF positive objects. Cross-linking of films increased the presence of this marker. The lowest contribution of VWF positive objects was found on the 2x cross-linked and 4x cross-linked films with HUVECs (Fig. 7C).

A similar tendency was observed for adhesion of the platelet-based aggregates (Fig. 7B). It was found that their contribution is almost three times higher for films without HUVECs than for coatings with cells. All cellularized coatings promoted adhesion of a similar number of leukocyte-based aggregates (Fig. 7D). Among them, the smallest adhesion was reported to the unmodified films.

4. Conclusions

The work presents the original results of interactions between polysaccharide-based films, endothelial cells and blood morphotic elements. The obtained results allowed us to show for the first time that the elastic modulus of PEMs influences endothelial cells functionality, namely free radical generation and as a consequence has an impact on the platelet aggregation mechanism. We have found that endothelial cells produced more free radicals on the coatings with elastic moduli between 40 kPa and 100 kPa. Moreover, we have found significantly lower adhesion of activated platelets and aggregates to the endothelium on the PEMs with elastic moduli above 40 kPa compared to coating variants with the lower Young moduli. Furthermore, the highest elastic moduli were correlated with the highest level of active platelets and aggregates circulating in blood. The observed blood-PEM interactions strongly correlate to the film elastic properties. In order to shed more light on the observed phenomenon we have investigated changes in the level of the Von Willebrand Factor, which is an important protein for platelet aggregation. We have found that the level of the VWF and number of platelet aggregates at the surface decreased with increasing film Young moduli. The opposite effect was observed in the blood from above the coatings. Films with elastic moduli above 40 kPa promoted increase in the VWF level and number of aggregates in the blood, which corresponds to a low percentage of the platelet aggregates at the surface.

Another type of protein, crucial for the platelets adhesion and activation, is P-selectin. It has been reported that expression of P-selectin by the endothelial cells supports the rolling of platelet aggregates at the endothelium surface [28,29]. Furthermore, it was found that P-selectin can determine size and stability of the aggregates[30]. Herein, the expression of the P-selectin was found to be the lowest at the surface of

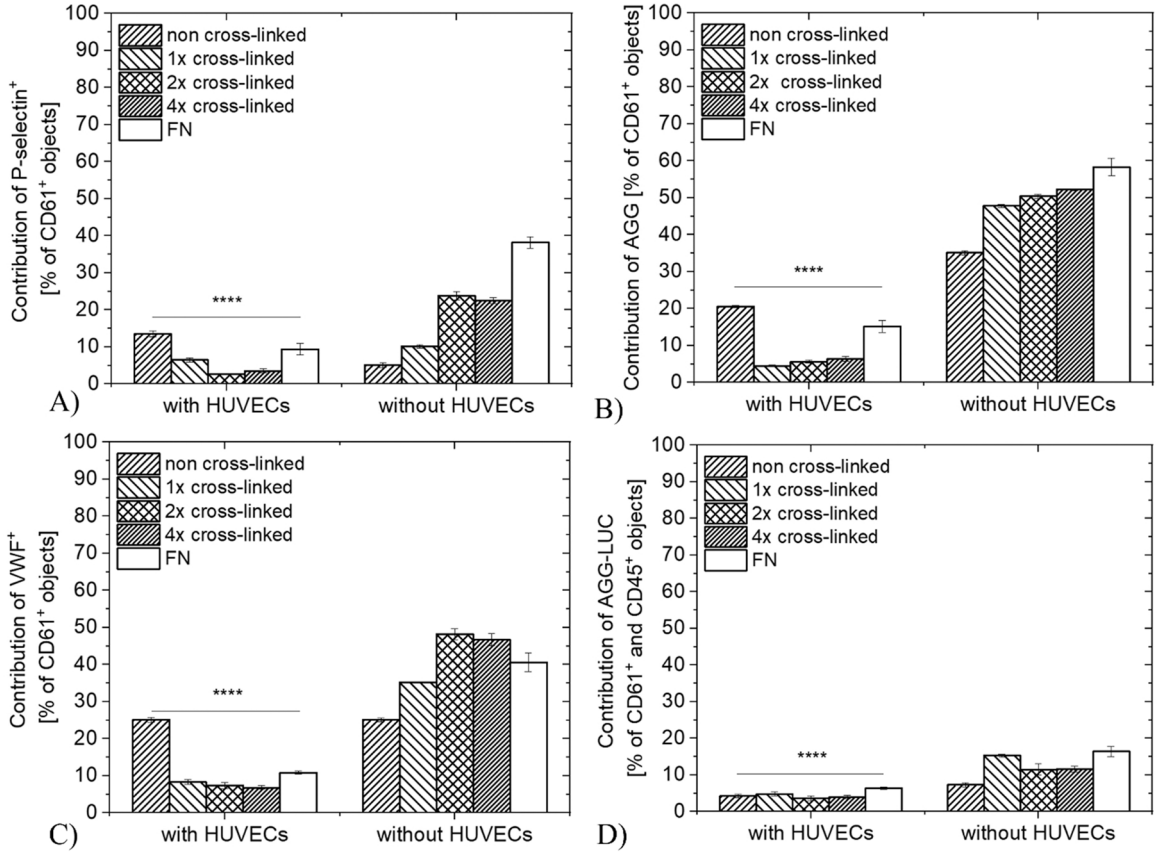

Fig. 7. PEM surface coverage by blood morphotic elements: A) P-selectin positive objects (P-selectin^{+}), B) platelet-based aggregates (AGG), C) von Willebrand Factor positive objects (VWF^{+}) and D) leukocyte-platelet aggregates (AGG-LUC). Data was represented as mean±SD. * ** *$p < 0.0001$ vs. corresponding coating without HUVECs.

the 2x and 4x cross-linked coatings. Simultaneously, the same coating types resulted in the highest P-selectin levels corresponding to the number of activated platelets and number of aggregates in the blood.

We postulate that differences in the platelet aggregation and adhesion to the PEMs of various elastic moduli may be explained by the rolling and two-stage aggregation mechanism described in our previous work [31]. The observations made for the >40 kPa coating corresponds to the rolling mechanism. This process includes soluble and immobilised VWF, which recruits platelets and binds $GPIb_{\alpha}$ during blood flow, whereas platelet activation is negligible [32]. Different behaviour was found for films with elastic moduli <40 kPa. This type of coatings showed a low level of active platelets and aggregates in blood simultaneously expressing higher levels of active surface platelets. Therefore, we suggest that on relatively softer films platelet aggregation follows a two-stage mechanism. During the blood flow, the high level of platelet activation molecules, i.e., P-selectin determines the formation of fibronectin-platelet integrin ($\alpha_{IIb}\beta_3$) complex, responsible for platelet aggregation. Contrarily, the VWF-$GPIb_{\alpha}$ complex forms rigid aggregates strongly attached to the surface. Graphical visualisation of both aggregation mechanisms is presented in Supplementary Information Fig. 2. We postulate that the observed transition between mechanisms of blood morphotic interaction with endothelial layers is the result of dynamic changes in the free radical generation.

To deeply understand the presented discovery and its correlation to free radical generation further investigation needs to be conducted. The next step should focus on detection of FR in *in vivo* dynamic blood-PEM-endothelium interaction experiment and also reflect to other factors responsible for blood morphotic elements functionality introducing co culture of endothelial and smooth muscle cells.

CRediT authorship contribution statement

Conceptualization, G.ImbirA.Mzyk, Methodology, G.ImbirA.Mzyk. SoftwareG.ImbirA.MzykK.Trembecka-Wojciga. Validation. G.ImbirA.MzykK.Trembecka-Wójciga. Formal analysis. G.ImbirA.MzykK.Trembecka-WójcigaP.Ozga. Investigation. G.ImbirK.Trembecka-WójcigaP.Ozga. Resources. A.MzykR.Schirhagl. Data Curation. G.ImbirA.Mzyk. Writing - Original Draft. G.ImbirA.Mzyk. Writing - Review & Editing. G.ImbirA.Mzyk and R.Schirhagl. Visualization. G.ImbirA.Mzyk. Supervision. A.Mzyk. Project administration. A.MzykG.Imbir. Funding acquisition. A.Mzyk, R.Schirhagl, G.Imbir.

Declaration of Competing Interest

The authors declare that they have no known competing financial interests or personal relationships that could have appeared to influence the work reported in this paper.

Data Availability

The authors do not have permission to share data.

Acknowledgments

The PEM coatings were manufactured and characterised thanks to a project financed by the National Centre of Science in Poland, grant No. 2014/15/N/ST8/02601 of the Polish National Center of Science. The PEM characterization was also supported by The European Virtual Institute on Knowledge-based Multifunctional Materials AISBL (KMM-VIN) Research Fellowship Call 2020 (Gabriela Imbir, Francesco Baino). Blood-material interaction experiments were supported by the European Union from resources of the European Social Fund (Project No. WND-POWR.03.02.00-00-I043/16).

Appendix A. Supporting information

Supplementary data associated with this article can be found in the online version at doi:10.1016/j.colsurfb.2023.113269.

References

[1] N. Tran, T.J. Webster, Nanotechnology for bone materials, Wiley Interdiscip. Rev. Nanomed. Nanobiotechnol. (2009), https://doi.org/10.1002/wnan.23.
[2] C.W. Cheng, L.D. Solorio, E. Alsberg, Decellularized tissue and cell-derived extracellular matrices as scaffolds for orthopaedic tissue engineering, Biotechnol. Adv. (2014), https://doi.org/10.1016/j.biotechadv.2013.12.012.
[3] S. Yamanlar, S. Sant, T. Boudou, C. Picart, A. Khademhosseini, Surface functionalization of hyaluronic acid hydrogels by polyelectrolyte multilayer films, Biomaterials (2011), https://doi.org/10.1016/j.biomaterials.2011.04.030.
[4] V. Gribova, R. Auzely-Velty, C. Picart, Polyelectrolyte multilayer assemblies on materials surfaces: From cell adhesion to tissue engineering, Chem. Mater. (2012), https://doi.org/10.1021/cm2032459.
[5] C. Picart, Polyelectrolyte multilayer films: from physico-chemical properties to the control of cellular processes, Curr. Med. Chem. (2008), https://doi.org/10.2174/092986708783885219.
[6] L. Richert, P. Lavalle, E. Payan, X.Z. Shu, G.D. Prestwich, J.F. Stoltz, P. Schaaf, J. C. Voegel, C. Picart, Layer by layer buildup of polysaccharide films: physical chemistry and cellular adhesion aspects, Langmuir (2004), https://doi.org/10.1021/la035415n.
[7] A. Mzyk, J.M. Lackner, P. Wilczek, L. Lipińska, A. Niemiec-Cyganek, A. Samotus, M. Morenc, Polyelectrolyte multilayer film modification for chemo-mechano-regulation of endothelial cell response, RSC Adv. 6 (2016), https://doi.org/10.1039/C5RA23019E.
[8] E. Guzmán, R.G. Rubio, F. Ortega, A closer physico-chemical look to the Layer-by-Layer electrostatic self-assembly of polyelectrolyte multilayers, Adv. Colloid Interface Sci. 282 (2020), https://doi.org/10.1016/J.CIS.2020.102197.
[9] P. Hamerli, T. Weigel, T. Groth, D. Paul, Surface properties of and cell adhesion onto allylamine-plasma-coated polyethylenterephtalat membranes, Biomaterials (2003), https://doi.org/10.1016/S0142-9612(03)00312-0.
[10] A. Schneider, G. Francius, R. Obeid, P. Schwinté, J. Hemmerlé, B. Frisch, P. Schaaf, J.C. Voegel, B. Senger, C. Picart, Polyelectrolyte multilayers with a tunable young's modulus: Influence of film stiffness on cell adhesion, Langmuir (2006), https://doi.org/10.1021/la0521802.
[11] P.H. Chua, K.G. Neoh, E.T. Kang, W. Wang, Surface functionalization of titanium with hyaluronic acid/chitosan polyelectrolyte multilayers and RGD for promoting osteoblast functions and inhibiting bacterial adhesion, Biomaterials (2008), https://doi.org/10.1016/j.biomaterials.2007.12.019.
[12] S.T. Dubas, P. Kittitheeranun, R. Rangkupan, N. Sanchavanakit, P. Potiyaraj, Coating of polyelectrolyte multilayer thin films on nanofibrous scaffolds to improve cell adhesion, J. Appl. Polym. Sci. (2009), https://doi.org/10.1002/app.30690.
[13] H. Kerdjoud, C. Boura, V. Moby, K. Montagne, P. Schaaf, J.C. Voegel, J.F. Stoltz, P. Menu, Re-endothelialization of human umbilical arteries treated with polyelectrolyte multilayers: A tool for damaged vessel replacement, Adv. Funct. Mater. (2007), https://doi.org/10.1002/adfm.200600795.
[14] M. Hamilos, S. Petousis, F. Parthenakis, Interaction between platelets and endothelium: from pathophysiology to new therapeutic options, Cardiovasc. Diagn. Ther. (2018), https://doi.org/10.21037/cdt.2018.07.01.
[15] G. Imbir, A. Mzyk, K. Trembecka-Wójciga, E. Jasek-Gajda, H. Plutecka, R. Schirhagl, R. Major, Polyelectrolyte multilayer films modification with ag and rgo influences platelets activation and aggregate formation under in vitro blood flow, Nanomaterials (2020), https://doi.org/10.3390/nano10050859.
[16] R. Sharmin, T. Hamoh, A. Sigaeva, A. Mzyk, V.G. Damle, A. Morita, T. Vedelaar, R. Schirhagl, Fluorescent nanodiamonds for detecting free-radical generation in real time during shear stress in human umbilical vein endothelial cells 6 (2021), https://doi.org/10.1021/acssensors.1c01582.
[17] A. Morita, T. Hamoh, F.P. Perona Martinez, M. Chipaux, A. Sigaeva, C. Mignon, K. J. Van Der Laan, A. Hochstetter, R. Schirhagl, The fate of lipid coated and uncoated fluorescent nanodiamonds during cell division in yeast, Nanomaterials (2020), https://doi.org/10.3390/nano10030516.
[18] S.R. Hemelaar, P. De Boer, M. Chipaux, W. Zuidema, T. Hamoh, F. Perona Martinez, A. Nagl, J.P. Hoogenboom, B.N.G. Giepmans, R. Schirhagl, Nanodiamonds as multi-purpose labels for microscopy, Sci. Rep. (2017), https://doi.org/10.1038/s41598-017-00797-2.
[19] M. Sanak, B. Jakiela, W. Wegrzyn, Assessment of hemocompatibility of materials with arterial blood flow by platelet functional tests, Bull. Pol. Acad. Sci. Tech. Sci. (2010), https://doi.org/10.2478/v10175-010-0029-z.
[20] T. Crouzier, T. Boudou, C. Picart, Polysaccharide-based polyelectrolyte multilayers, Curr. Opin. Colloid Interface Sci. (2010), https://doi.org/10.1016/j.cocis.2010.05.007.
[21] J. Almodóvar, L.W. Place, J. Gogolski, K. Erickson, M.J. Kipper, Layer-by-layer assembly of polysaccharide-based polyelectrolyte multilayers: a spectroscopic study of hydrophilicity, composition, and ion pairing, Biomacromolecules (2011), https://doi.org/10.1021/bm200519y.
[22] L. Mhamdi, C. Picart, C. Lagneau, A. Othmane, B. Grosgogeat, N. Jaffrezic-Renault, L. Ponsonnet, Study of the polyelectrolyte multilayer thin films' properties and correlation with the behavior of the human gingival fibroblasts, Mater. Sci. Eng. C (2006), https://doi.org/10.1016/j.msec.2005.10.049.

[23] J. Lee, A. Ishihara, G. Oxford, B. Johnson, K. Jacobson, Regulation of cell movement is mediated by stretch-activated calcium channels, Nature (1999), https://doi.org/10.1038/22578.
[24] C.M. Lo, H.B. Wang, M. Dembo, Y.L. Wang, Cell movement is guided by the rigidity of the substrate, Biophys. J. (2000), https://doi.org/10.1016/S0006-3495(00)76279-5.
[25] P. Karki, A.A. Birukova, Substrate stiffness-dependent exacerbation of endothelial permeability and inflammation: mechanisms and potential implications in ALI and PH (2017 Grover Conference Series), Pulm. Circ. (2018), https://doi.org/10.1177/2045894018773044.
[26] R. Krishnan, D.D. Klumpers, C.Y. Park, K. Rajendran, X. Trepat, J. Van Bezu, V.W. M. Van Hinsbergh, C.V. Carman, J.D. Brain, J.J. Fredberg, J.P. Butler, G.P. Van Nieuw Amerongen, Substrate stiffening promotes endothelial monolayer disruption through enhanced physical forces, Am. J. Physiol. - Cell Physiol. (2011), https://doi.org/10.1152/ajpcell.00195.2010.
[27] M. Hu, H. Chang, H. Zhang, J. Wang, W.X. Lei, B.C. Li, K.F. Ren, J. Ji, Mechanical adaptability of the MMP-responsive film improves the functionality of endothelial cell monolayer, Adv. Healthc. Mater. (2017), https://doi.org/10.1002/adhm.201601410.
[28] Z.M. Ruggeri, Von Willebrand factor, platelets and endothelial cell interactions, J. Thromb. Haemost. (2003), https://doi.org/10.1046/j.1538-7836.2003.00260.x.
[29] P.S. Frenette, R.C. Johnson, R.O. Hynes, D.D. Wagner, Platelets roll on stimulated endothelium in vivo: an interaction mediated by endothelial P-selectin, Proc. Natl. Acad. Sci. U. S. A. (1995), https://doi.org/10.1073/pnas.92.16.7450.
[30] M. Merten, P. Thiagarajan, P-selectin expression on platelets determines size and stability of platelet aggregates, Circulation (2000), https://doi.org/10.1161/01.CIR.102.16.1931.
[31] A. Mzyk, G. Imbir, K. Trembecka-Wójciga, J.M. Lackner, H. Plutecka, E. Jasek-Gajda, J. Kawałko, R. Major, Rolling or two-stage aggregation of platelets on the surface of thin ceramic coatings under in vitro simulated blood flow conditions, ACS Biomater. Sci. Eng. 6 (2020), https://doi.org/10.1021/acsbiomaterials.9b01074.
[32] B. Savage, E. Saldívar, Z.M. Ruggeri, Initiation of platelet adhesion by arrest onto fibrinogen or translocation on von Willebrand factor, Cell (1996), https://doi.org/10.1016/S0092-8674(00)80983-6.